Supplementary Information for:

Assessment of inter-city transport of particulate matter in the Beijing-Tianjin-Hebei region

X. Chang[1], S. X. Wang[1,2], B. Zhao[3], S. Y. Cai[1], and J. M. Hao[1,2]

[1] State Key Joint Laboratory of Environment Simulation and Pollution Control, School of Environment, Tsinghua University, Beijing 100084, China

[2] State Environmental Protection Key Laboratory of Sources and Control of Air Pollution Complex, Beijing 100084, China

[3] Joint Institute for Regional Earth System Science and Engineering and Department of Atmospheric and Oceanic Sciences, University of California, Los Angeles, CA 90095, USA

Correspondence to: S. X. Wang [shxwang@tsinghua.edu.cn]
and B. Zhao [zhaob1206@ucla.edu]

1. Spatial distribution of emission

Figure S1 shows the spatial distribution of three main pollutants, i.e. $PM_{2.5}$, NOx and SO_2, in the BTH region. The emissions are allocated into grids with GDP, population or road patterns, based on different emission sectors.

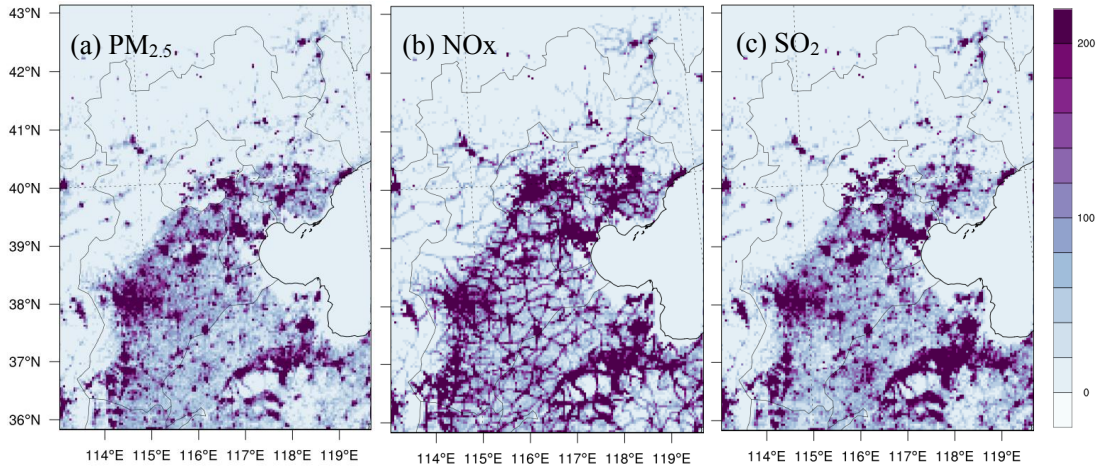

Figure S1 Spatial distribution of the emission of (a) $PM_{2.5}$, (b) NOx and (c) SO_2 in the 4-km grid covering the BTH region. Units are all in t $year^{-1}$ $grid^{-1}$

2. Evaluation of the meteorology simulation

The simulated meteorological fields are evaluated by the observation data in the BTH region. The observational data of meteorology are from the National Climatic Data Center (NCDC) of NOAA (www.ncdc.noaa.gov), where observations of every 3 hours in 78 international exchange sites in the BTH region are provided. The statistical indices used for evaluation include the bias and gross error (GE) between observation and simulation with regard to wind speed at 10 m, temperature at 2 m, and specific humidity at 2 m. The bias and GE are defined as

$$\text{bias} = \frac{\sum_1^n (\text{SIM} - \text{OBS})}{n} \quad (1)$$

$$\text{GE} = \frac{\sum_1^n |\text{SIM} - \text{OBS}|}{n} \quad (2)$$

where n is the total number of observation and simulation data pairs, and SIM and OBS stand for individual simulated and observed values

respectively. The parameters evaluated include wind speed at 10 m (WS10), wind direction at 10 m (WD10), temperature at 2 m (T2), and specific humidity at 2 m (Q2). The results are shown in Table S1. The WS10, T2, and Q2 simulations all agree well with observations under the benchmark suggested by Emery (2011). The bias of WD10 also falls within the benchmark, but the gross error exceeds the benchmark for both January and July. The larger gross error is partly caused by the lower precision of the observation data. The WD10 observations only have 16 different values, while the simulation could have any value between 0 and 360. For example, if the real WD10 is 125 degree, the value will be reported as 140 degree. Even if the simulation is exactly 125 degree, an additional gross error of 15 degree will be introduced. In addition, compared to other similar simulation studies in China (e.g., Hu et al., 2016; Zhao et al., 2013), the gross error of WD10 falls in a similar range.

Table S1 Comparison of simulated and observed meteorology parameters.

Parameter	Indice	Unit	Benchmark[a]	Jan-2012	Jul-2012
Wind speed (WS10)	Observation Mean	m s^{-1}	-	2.34	2.32
	Simulation Mean	m s^{-1}	-	2.59	2.51
	Bias	m s^{-1}	≤±0.5	-0.24	-0.20
	Gross error	m s^{-1}	≤2	1.12	1.08
Wind direction (WD10)	Observation Mean	deg	-	203.9	175.2
	Simulation Mean	deg	-	222.4	174.8
	Bias	deg	≤±10	-2.64	-1.47
	Gross error	deg	≤30	43.23	43.7
Temperature (T2)	Observation Mean	K	-	266.1	298.0
	Simulation Mean	K	-	266.2	297.8
	Bias	K	≤±0.5	-0.13	0.22
	Gross error	K	≤2	1.64	1.72
Humidity (Q2)	Observation Mean	g kg^{-1}	-	1.23	14.80
	Simulation Mean	g kg^{-1}	-	1.36	14.56
	Bias	g kg^{-1}	≤±1	-0.13	0.23
	Gross error	g kg^{-1}	≤2	0.29	1.53

a. The benchmarks used in this study are suggested by Emery (2011)

3. Comparison of the simulation and observation results for the major components of PM2.5

The simulation results of the major components of $PM_{2.5}$ are compared

with observations in Ling County and Xiong County from Jul. 22nd to Aug. 23rd. The results are shown in Figure S1. Some statistical indices including NMB and NME are calculated, as is shown in Table S2.

Table S2 Comparison of simulated and observed $PM_{2,5}$ and its major components in two sites from Jul, 22nd to Aug. 23rd, 2013.

Jul 22 ~ Aug 23, 2013		**Observation Mean**	**Simulation Mean**	**NMB**	**NME**
Unit		μg·m^{-3}	μg·m^{-3}	%	%
	Total $PM_{2.5}$	75.5	84.5	+11.9	36.9
	EC	2.76	6.07	+120	123.3
Xiong	OC	10.88	8.12	-25.4	33.0
County	Nitrate	11.6	22.7	+95.2	114.0
	Sulfate	20.7	9.87	-52.3	55.5
	Ammonium	10.1	10.3	+2.4	38.6
	Total $PM_{2.5}$	73.9	64.5	-7.5	37.4
	EC	1.70	3.43	+117	132.3
Ling	OC	6.09	5.76	-1.2	32.4
County	Nitrate	12.3	21.4	+78.6	92.1
	Sulfate	24.6	10.0	-56.6	58.6
	Ammonium	12.3	9.99	-14.2	40.8

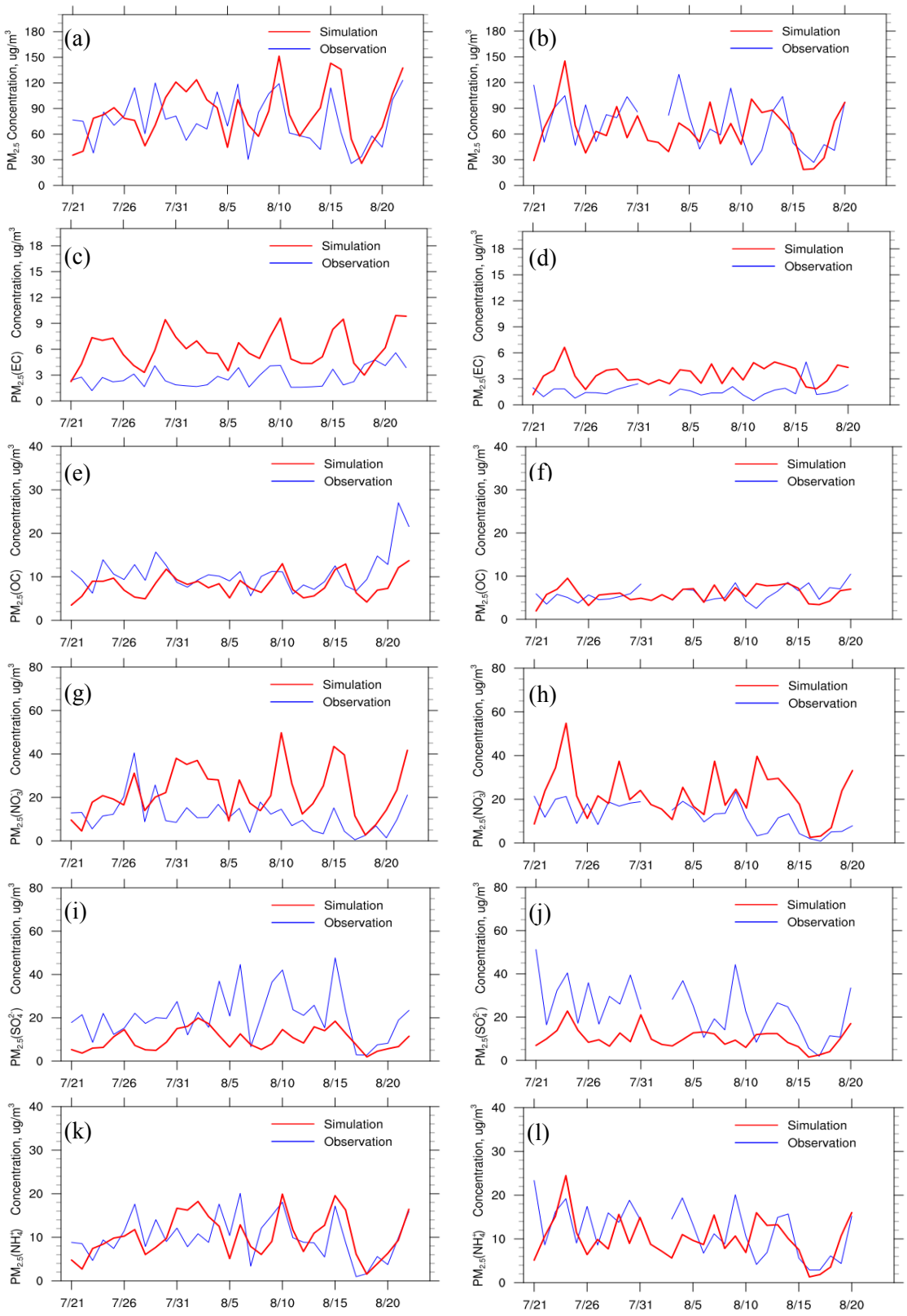

Figure S2 Time series of the simulation and observation of (a, b) $PM_{2.5}$, and its five major components: (c, d) EC, (e, f) OC, (g, h) nitrate, (i, j) sulfate and (k, l)ammonium in Xiong County (left) and Ling County (right) during Jul. 22nd to Aug. 23rd, 2013.

The model performance on the $PM_{2.5}$ major components are compared with other studies in the BTH region, shown in Table S3. All of the studies underestimate the sulfate concentrations. The underestimation ranges between 9% and 79%, and most of them are larger than 30%. The nitrate simulation results vary in different studies, but the majority of the studies tend to overestimate its concentration. The concentration of EC is usually much lower than the other four components, which may contribute to the large discrepancy in the simulation results in different studies. For OC, although some studies overestimate the concentration, more studies exhibit a lower concentration than observation. Generally speaking, the biases of the $PM_{2.5}$ components in the current study have similar magnitude to other recent studies in the BTH region.

Table S3 Summary of the $PM_{2.5}$ component simulation results for the BTH region in recent studies

Time	Site	SO_4^{2-} NMB (%)	NO_3^- NMB (%)	NH_4^+ NMB (%)	EC NMB (%)	OC NMB (%)	Reference
2005 annual	Tsinghua, Beijing	-14	13	10	-24	-36	Wang et al., 2011
2005 annual	Miyun, Beijing	-36	62	9	-17	-52	Wang et al., 2011
14 Jan – 8 Feb, 2010	Beijing	-72	-32	-5	124	26	Liu et al., 2016
14 Jan – 8 Feb, 2010	Shangdianzi, Beijing	-78	-24	-13	36	-7	Liu et al., 2016
Jan, 2010	Peking university, Beijing	-39	85	33	101	-2	Liu et al., 2016
14 Jan – 8 Feb, 2010	Shijiazhuang, Hebei	-79	-35	-7	81	38	Liu et al., 2016
14 Jan – 8 Feb, 2010	Chengde, Hebei	-78	48	-10	-39	-50	Liu et al., 2016
14 Jan – 8 Feb, 2010	Tianjin	-72	0	9	149	85	Liu et al., 2016
11-15 Jan, 2013	Beijing	~ -73	~ -43	-	-	-	Wang et al., 2014
Jan 2013	Handan, Hebei	-9	33	-11	50	37	Wang et al., 2015
Jul 2013	Handan, Hebei	-32	-3	8	96	30	Wang et al., 2015
Oct – Nov, 2014	7 sites in the BTH region	-48	16	-25	87	-37	Zhao et al., 2017
22 Jul – 23 Aug, 2012	Xiong County, Hebei	-52	95	2	120	-25	This study
22 Jul – 23 Aug, 2012	Ling County, Shandong	-57	79	-14	117	-1	This study

4. Wind rose plots for Tianjin and Shijiazhuang

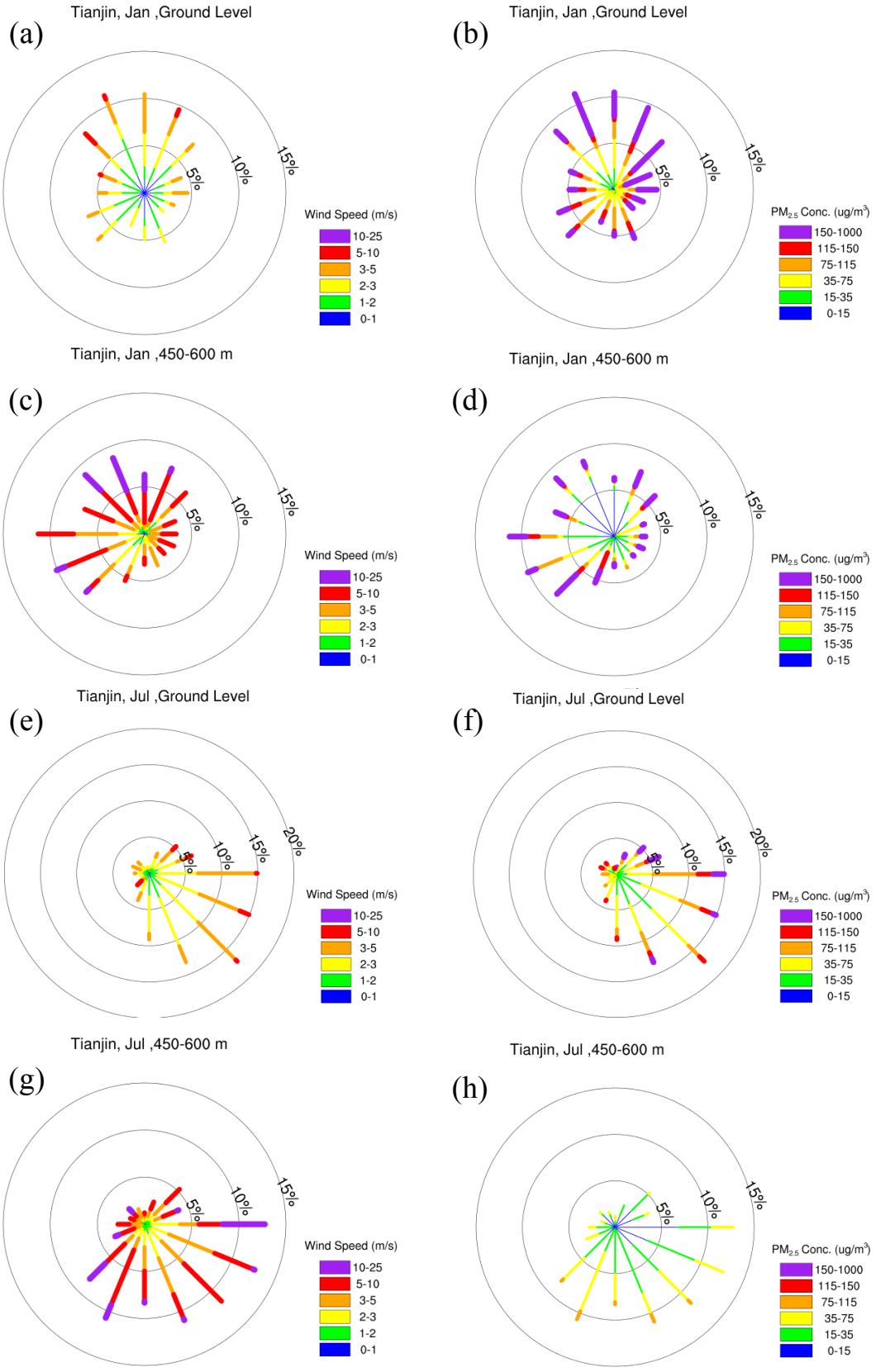

Figure S3 The wind rose plots showing the frequency of wind speed (a, c, e, g) and

$PM_{2.5}$ concentration (b, d, f, h) at different wind directions for Tianjin. The round level and the 7th level (about 450-600 m) in the model are chosen as the representation of lower levels and upper levels. The percentages denote the frequency.

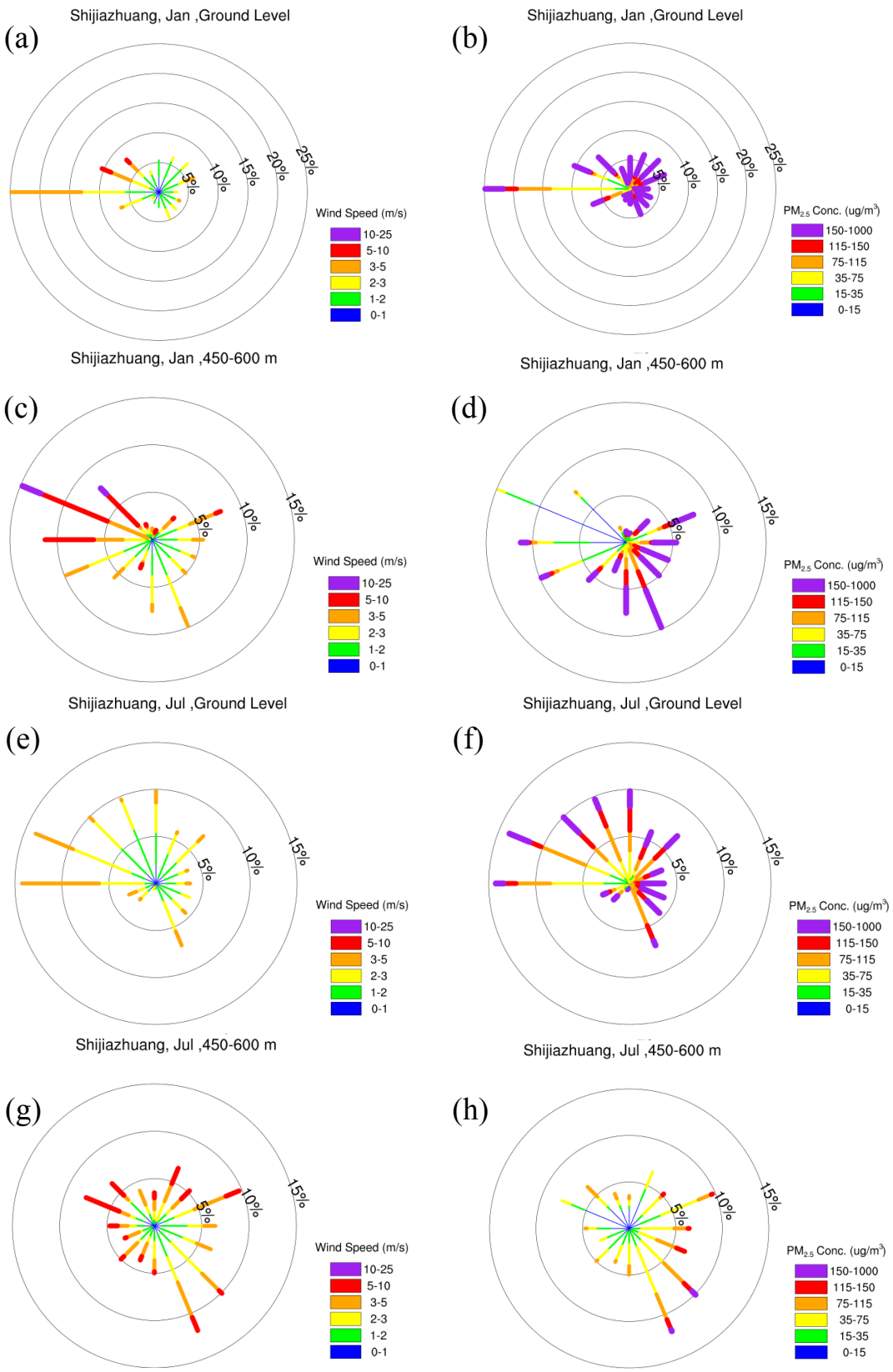

Figure S4 The wind rose plots showing the frequency of wind speed (a, c, e, g) and $PM_{2.5}$ concentration (b, d, f, h) at different wind directions for Shijiazhuang. The round level and the 7th level (about 450-600 m) in the model are chosen as the

representation of lower levels and upper levels. The percentages denote the frequency.

5. The influence of mountain-plain winds on the transport in Beijing

The simulated average diurnal wind patterns at 100 m height in January and July in Beijing are shown in Fig. S5(b). We also put the observation results from Tang et al., (2016) in Fig S5(a) as a reference. We find that the simulated wind pattern is consistent with the observation. In January, the mountain-plain winds are presented as the change in wind speed, but the wind direction does not change significantly during the whole day. In July, there is a significant wind direction shift, similar to the description of the reviewer. The mountainous wind (northeast) begins at 2:00 LT, and is taken over by the plain wind (southeast) at about 10:00 LT, and the mountainous wind is much weaker than the plain wind. A circulation of mountain-plain wind may have influence on the transport of $PM_{2.5}$ in July.

Considering that the mountain-plain wind circulation mainly happens at the foot of the mountains, we calculated the fluxes through the boundaries between Beijing and its three neighboring cities on the south/southeast (Baoding, Langfang and Tianjin) during mountainous wind hours and the plain wind hours in July separately (Fig. S6). During the plain wind hours, all the boundaries on the southwest and southeast of Beijing have positive net fluxes, which is due to the relatively strong southerly plain winds. During the mountainous wind hours, however, there is no significant

direction change of the fluxes except for the boundary of Baoding and Southern Langfang at levels below 200 m. The sign of fluxes mostly remaines unchanged because the mountain-plain wind circulation is weaker at higher levels, and the wind speed of the mountainous wind is even weaker at the southernly boundaries which has limited effect to alter the sign of the flux. Nevertheless, the magnitude of fluxes is significantly smaller than the plain wind hours, which is partly attributed to the mountain-plain wind circulation. Therefore, the summertime mountain-plain wind circulation in Beijing does not significantly alter the sign of inter-city $PM_{2.5}$ fluxes but does have considerable impact on their magnitude.

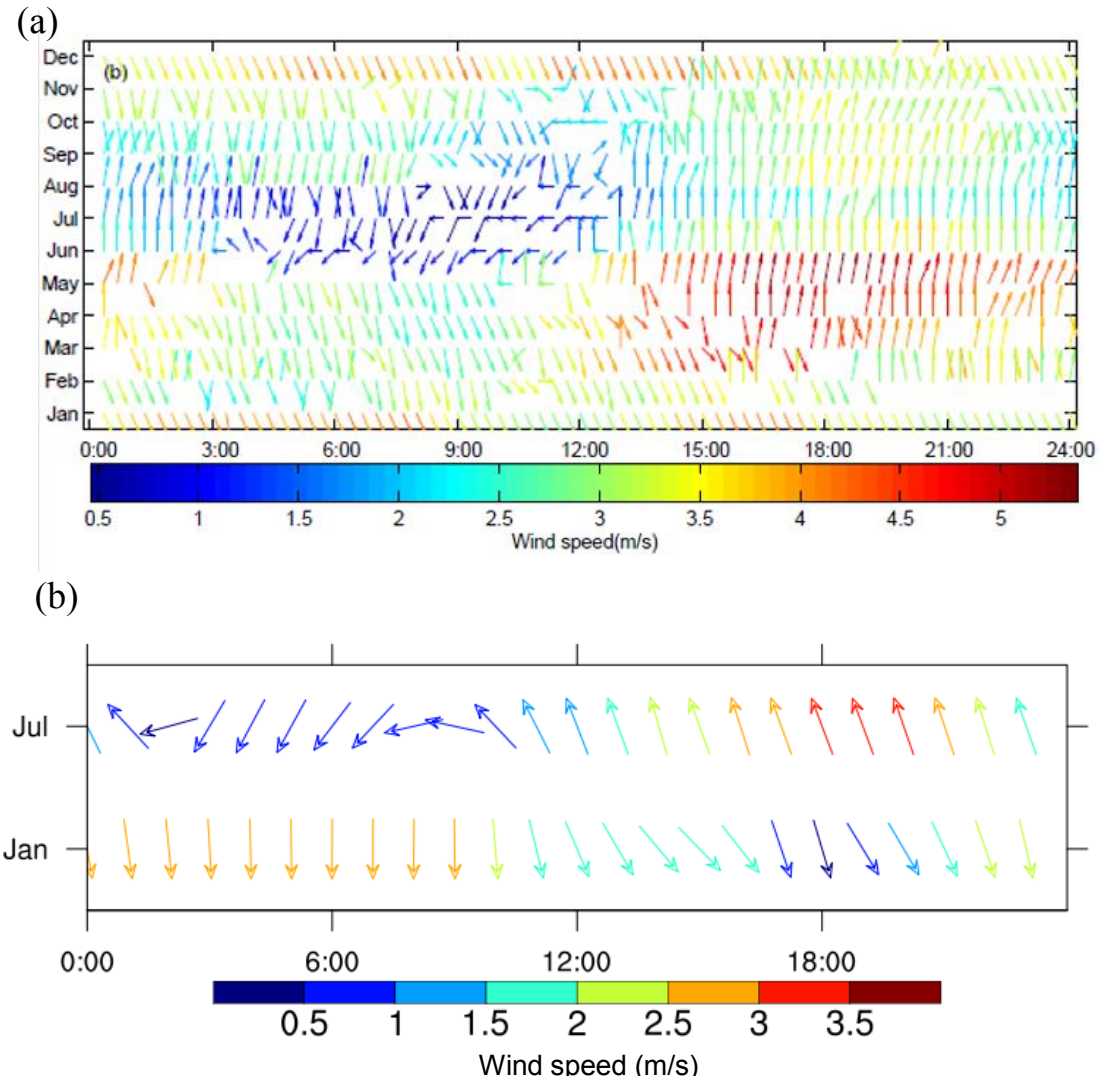

Figure S5 The observed and simulated monthly average diurnal variation of winds in Beijing in July. (a) The observation results from Tang et al. (2016). (b) The simulation results in this study.

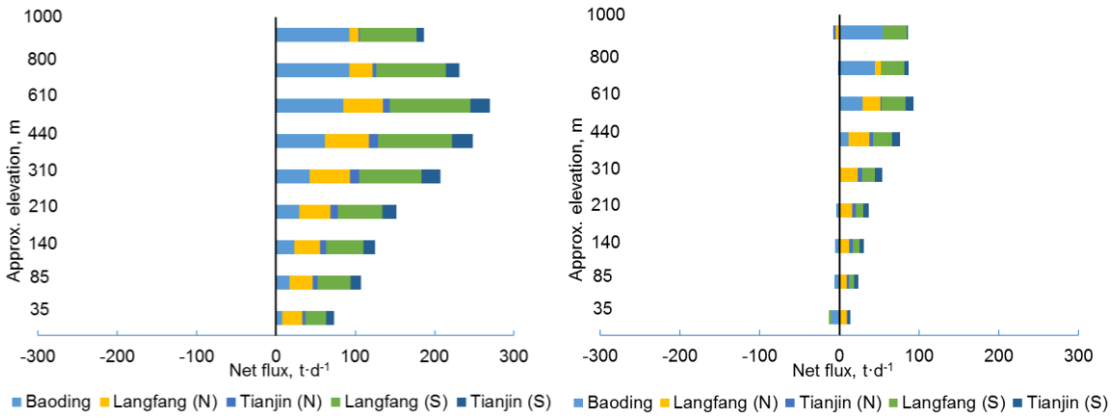

Figure S6 The transport fluxes in July between Beijing and its neighboring cities during (a) plain wind hours (11:00 – 1:00 (+1 day) LT) and (b) mountainous wind hours (2:00 – 10:00 LT)

References

Emery, C., Tai, E., and Yarwood, G.: Enhanced meteorological modeling and performance evaluation for two texas episodes, Prepared for the Texas Natural Resource Conservation Commission, by ENVIRON International Corp, Novato, CA, 2001.

Hu, J., Chen, J., Ying, Q., and Zhang, H.: One-year simulation of ozone and particulate matter in China using WRF/CMAQ modeling system, Atmospheric Chemistry and Physics, 16, 10333-10350, 10.5194/acp-16-10333-2016, 2016.

Kwok, R. H. F., Baker, K. R., Napelenok, S. L., and Tonnesen, G. S.: Photochemical grid model implementation and application of VOC, NOx, and O-3 source apportionment, Geoscientific Model Development, 8, 99-114, 10.5194/gmd-8-99-2015, 2015.

Liu, J., Mauzerall, D. L., Chen, Q., Zhang, Q., Song, Y., Peng, W., Klimont,

159 Z., Qiu, X. H., Zhang, S. Q., Hu, M., Lin, W. L., Smith, K. R., and
160 Zhu, T.: Air pollutant emissions from Chinese households: A major
161 and underappreciated ambient pollution source, P. Natl. Acad. Sci.
162 USA, 113, 7756–7761, 2016.
163 Tang, G., Zhang, J., Zhu, X., Song, T., Muenkel, C., Hu, B., Schaefer, K.,
164 Liu, Z., Zhang, J., Wang, L., Xin, J., Suppan, P., and Wang, Y.: Mixing
165 layer height and its implications for air pollution over Beijing, China,
166 Atmospheric Chemistry and Physics, 16, 2459-2475, 10.5194/acp-16-
167 2459-2016, 2016.
168 Wang, S., Xing, J., Chatani, S., Hao, J., Klimont, Z., Cofala, J., and Amann,
169 M.: Verification of anthropogenic emissions of China by satellite and
170 ground observations, Atmospheric Environment, 45, 6347-6358,
171 10.1016/j.atmosenv.2011.08.054, 2011.
172 Wang, L. T., Wei, Z., Yang, J., Zhang, Y., Zhang, F. F., Su, J., Meng, C. C.,
173 and Zhang, Q.: The 2013 severe haze over southern Hebei, China:
174 model evaluation, source apportionment, and policy implications,
175 Atmospheric Chemistry and Physics, 14, 3151-3173, 10.5194/acp-14-
176 3151-2014, 2014.
177 Wang, L., Wei, Z., Wei, W., Fu, J. S., Meng, C., and Ma, S.: Source
178 apportionment of PM2.5 in top polluted cities in Hebei, China using
179 the CMAQ model, Atmospheric Environment, 122, 723-736,
180 10.1016/j.atmosenv.2015.10.041, 2015.
181 Zhao, B., Wang, S., Wang, J., Fu, J. S., Liu, T., Xu, J., Fu, X., and Hao, J.:
182 Impact of national NOx and SO2 control policies on particulate matter

pollution in China, Atmospheric Environment, 77, 453-463, 10.1016/j.atmosenv.2013.05.012, 2013.

Zhao, B., Wu, W., Wang, S., Xing, J., Chang, X., Liou, K.-N., Jiang, J. H., Jang, C., Fu, J. S., Zhu, Y., Wang, J., and Hao, J.: A modeling study of the nonlinear response of fine particles to air pollutant emissions in the Beijing-Tianjin-Hebei region, Atmospheric Chemistry and Physics Discussions, 10.5194/acp-2017-428, 2017.